A proteomic analysis of chemoresistance development via sequential treatment with doxorubicin reveals novel players in MCF-7 breast cancer cells

ANN-KATRIN SOMMER[1], ADAM HERMAWAN[1], BOJAN LJEPOJA[1], THOMAS FRÖHLICH[2], GEORG J. ARNOLD[2], ERNST WAGNER[1] and ANDREAS ROIDL[1]

[1]Pharmaceutical Biotechnology, Department of Pharmacy; [2]Laboratory for Functional Genome Analysis (LAFUGA), Gene Center, Ludwig-Maximilians-Universität München, D-81377 Munich, Germany

Abstract. Breast cancer exhibits the highest incidence of all cancer types and is the 2nd leading cause of cancer mortality in women. Up to 82% of breast cancer patients receive a chemotherapy-containing treatment regimen. However, numerous breast tumors recur within 10 years following an initial response and are frequently resistant to previous therapeutic agents. Thus, to analyze the crucial factors, and whether the development of resistance in tumor cells follows certain patterns, is of great importance. In the present study, the clinical treatment schedule of the frequently used chemotherapeutic drug doxorubicin was applied in an *in vitro* model, the Molecular Evolution Assay (MEA), leading to resistance formation. By investigating the alterations in protein expression in MCF-7 breast cancer cells with three biological replicates, it was observed that the development of resistance to doxorubicin is a multi-directed process. The number and composition of the differentially expressed proteins varied, in addition to the pathways involved in chemoresistance, leading to only a small number of proteins and pathways being commonly regulated in all the MEAs. The proteins 60S ribosomal export protein NMD3 and 4F2 cell-surface antigen heavy chain (SLC3A2) were identified to be the most promising differentially expressed targets; the gene ontology term 'apoptotic signaling pathway' was reduced and 'cell redox homeostasis'

Correspondence to: Dr Andreas Roidl, Pharmaceutical Biotechnology, Department of Pharmacy, Ludwig-Maximilians-Universität München, Butenandtstrasse 5-13, D-81377 Munich, Germany
E-mail: andreas.roidl@cup.uni-muenchen.de

was upregulated. Based on the present findings *in vitro*, it may be hypothesized that the development of resistance in patients is an even more complex process, emphasizing the need for further investigations of resistance development in the clinic to eventually improve patient outcomes.

Introduction

According to the American Cancer Society and the International Agency for Research on Cancer, breast cancer has the highest incidence of all cancer types in women worldwide (1,2). Furthermore, breast cancer is the 2nd leading cause of cancer mortality in the United States, where 38 to 82% of breast cancer patients, depending on stage, receive chemotherapy in adjuvant and neoadjuvant treatment regimens (3). One of the most frequently used chemotherapeutics in breast cancer therapy is doxorubicin (DXR). This drug belongs to the anthracycline antibiotic family and was isolated from *Streptomyces peucetius* (4). It acts by binding topoisomerase II (5), via DNA intercalation (6) and by generating free radicals (7), resulting in DNA damage (8-12). A major obstacle in the treatment of breast cancer is the recurrence of the tumor. According to the Early Breast Cancer Trialists' Collaborative Group, 39.4% of breast tumors previously treated with anthracyclines recur within 10 years (13). A majority of relapses are resistant to the previous chemotherapeutic drugs resulting in a poor prognosis for patients with breast cancer. In general, there are two hypotheses explaining the development of chemoresistance: The cancer stem cell (CSC) model and the clonal evolution model (14-19). The CSC model is based on the hypothesis that solid tumor cells are hierarchically organized with CSCs at the apex, followed by fast proliferating progenitors and, finally, differentiated cancer cells. CSCs are capable of indefinite self-renewal, give rise to aberrant differentiated cells and are intrinsically resistant to chemotherapy (14). The clonal evolution model, on the other hand, states that tumor cells are stochastically organized and that tumor progression is driven by the fittest clone and not by CSCs (15). Since genomic instability is one hallmark of cancer (20), mutations in the tumor cells occur spontaneously. A subsequent selection pressure or a biological advantage leads to the propagation

of certain cell clones (15). One example of a strong selection pressure is chemotherapeutic drugs, including DXR, which kill the majority of cancer cells, although certain resistant clones survive, giving rise to a new tumor cell population that is insensitive to the drug used previously (21,22).

Previous studies demonstrated that DXR-resistant cancer cells exhibit activated DNA damage repair mechanisms (23), alterations in topoisomerase II expression (24), overexpression of drug metabolizing enzymes (25,26), mutations in cellular tumor antigen p53 (27) and, particularly, enhanced drug efflux mediated by transporters belonging to the ATP-binding cassette superfamily (28,29). However, all of the *in vitro* studies dealing with DXR resistance have analyzed resistant cells which were permanently maintained in DXR-containing medium. In the clinical setting, however, chemotherapy with DXR is usually applied in four cycles of 60 mg/m^2 every 3rd week, in combination with cyclophosphamide (13). Recovery phases of ≤2 weeks in between are an important part of the therapy to allow the patient to cope with the toxic drugs.

Therefore, the aim of the present study was to investigate the development of resistance by treating breast cancer cells for five rounds with DXR, and including treatment-free periods in between, thus mimicking the clinical therapy regimen of patients. This assay was termed the Molecular Evolution Assay (MEA), as it was possible to observe alterations in the protein expression upon a selection pressure (in this case, DXR) over time. This assay may reflect the development of acquired resistance in a more realistic way compared with constant high-dose drug treatments. Three independent MEAs (A, B and C) were performed in the breast cancer cell line MCF-7 to address the question of whether resistance formation follows similar patterns upon the same selection pressure, and to identify its crucial factors. Thus, the present study analyzed different biological replicates under the same conditions. In order to investigate the alterations in protein expression during resistance formation, a proteomics approach using liquid chromatography-mass spectrometry (LC-MS) was performed. This technique revealed differentially expressed proteins by comparing untreated cells with cells treated three and five times, thus elucidating important mechanisms of resistance formation.

Materials and methods

Cell culture. The breast cancer cell line MCF-7 was obtained from CLS Cell Lines Service GmbH (Eppelheim, Germany) and cultured in Dulbecco's modified Eagle's medium high glucose (Sigma-Aldrich; Merck KGaA, Darmstadt, Germany) containing 10% fetal calf serum (Gibco; Thermo Fisher Scientific, Inc., Waltham, MA, USA) at 37°C and 5% CO$_2$. For the following experiments, cells were used at passage number 5 (MEA A), 7 (MEA B) and 8 (MEA C), respectively.

MEA. The MEA was performed as described previously (30). MCF-7 cells were treated with 50 nM DXR (Sigma-Aldrich; Merck KGaA) for 72 h. Subsequently, the drug was removed and the remaining cells were cultured until they reached a confluence of 80%. Finally, the cells were split and 4 days subsequently one dish was taken for the next treatment round, one for proteomics analysis and one for cell viability

measurements. The rounds 0 (R0), 3 (R3) and 5 (R5) were used for proteomics analysis. This experiment was performed three times independently.

Cell viability assay. To assess the resistance formation of R3 and R5 compared with R0, a CellTiter Glo Assay (Promega Corporation, Madison, WI, USA) was performed. Untreated cells, three times DXR-treated and five times DXR-treated cells were seeded in triplicates (3,000 cells/well), treated with 1 μM DXR for 72 h and were analyzed subsequently using a luminometer (Berthold Technologies GmbH & Co. KG, Bad Wildbad, Germany), according to the manufacturer's protocol.

Protein lysis. For protein lysis, cells were seeded at a density of 80%, washed three times with cold PBS and subsequently harvested using a protein lysis buffer containing 8 M urea and 400 mM ammonium bicarbonate. To improve cell lysis, ultrasound was used and samples were centrifuged through QIA-shredder devices (Qiagen GmbH, Hilden, Germany) at 2,800 x g for 1 min at room temperature. A total of 20 μg protein was used for subsequent reduction with 45 mM dithio-erythritol (DTE) and for alkylation with 0.1 M iodoacetamide, both performed for 30 min at room temperature. Finally, samples were trypsinized at 37°C overnight using 400 ng porcine trypsin.

LC-MS. Peptide separation and identification was performed on an EASY-nLC 1000 chromatography system (Thermo Fisher Scientific, Inc.) coupled to an Orbitrap XL instrument (Thermo Fisher Scientific, Inc.). A total of 2.5 μg peptides was diluted in 10 μl 0.1% formic acid and injected on a trap column (PepMap100 C18; 75 μm x2 cm; 3 μm particles; Thermo Fisher Scientific, Inc.).

Chromatography was performed at a flow rate of 200 nl/min at 40°C (column, PepMap RSLC C18; 75 μm x50 cm; 2 μm particles; Thermo Fisher Scientific, Inc.) with a 260-min linear gradient of 5-25% solvent B (0.1% formic acid; 100% acetonitrile) and a subsequent 60-min gradient of 25-50% solvent B. MS spectra were acquired using a top five data dependent collision-induced dissociation method. Mass spectra were acquired in parallel mode performing the precursor mass scanning in the Orbitrap (60,000 full width at half maximum resolution at m/z 400; 300-2,000 m/z), and five data dependent collision-induced dissociation tandem MS scans (dynamic exclusion activated) in the LTQ ion trap at a collision energy of 35%.

Bioinformatics. The mass spectrometry data were processed using MaxQuant 1.5.1.0 (31). To analyze the MS data, the Perseus module of the MaxQuant software was used (32). For the following investigations the label free quantification value of the identified proteins was used and proteins that were identified as potential contaminants or only identified by site were excluded. Subsequently, the values were transformed applying the logarithm to base 2.

For the multiscatter blot, the R0s of each MEA were compared with each other to identify the initial perturbation of protein expression at different passage numbers (5, 7 and 8) of MCF-7 cells. Therefore, two valid values in at least one MEA were required and the missing values were replaced from a

normal distribution using the imputation feature of Perseus (width, 0.3; down-shift, 1.8). Subsequently, the median of each MEA was calculated and the R0s of the different MEAs were compared with each other applying a Pearson correlation analysis (Perseus module of the MaxQuant software). The same analysis was used to compare the different R3s and R5s.

A gene set enrichment analysis (GSEA) was performed to evaluate alterations in signaling pathways. All MEAs were grouped to investigate the overall abundance alterations in R3 and R5 compared with R0. Subsequently, each MEA was analyzed separately and the measurement replicates were grouped. Only proteins that were identified twice in at least one group were further investigated. The missing values were replaced from a normal distribution. The resulting values were analyzed with gsea2-2.2.3 from the Broad Institute (Cambridge, MA, USA) (33,34). The gene set database gene ontology biological process (GO_BP) (35) was used, and as metric for ranking genes the t-test was chosen. The global enrichment score (ES) reflects the degree to which a defined set of genes is overrepresented at the top or the bottom of the entire ranked gene list, and it corresponds to a weighted Kolmogorov-Smirnov-like statistic.

Subsequently, the MEAs A, B and C were examined separately to evaluate the differentially expressed proteins. The three measurement replicates of R0, R3 and R5 were grouped and two valid values in at least one group were required for further investigation. The missing values were replaced applying the aforementioned imputation feature of Perseus to allow for statistical evaluation. In the present study, a two-tailed and paired Student's t-test with a false discovery rate of 0.05 was performed to compare R0 with R3 and R0 with R5 using the Perseus module of the MaxQuant software. To identify upregulated and downregulated proteins they were sorted according to their t-test difference, and values >0 were regarded as increased and <0 as decreased protein expression. Following this, Venn analysis was performed to determine the common regulated proteins in MEA A, B and C. Venny 2.1 was utilized (36). Finally, the common regulated proteins were compared by Venn analysis to identify proteins which were upregulated or downregulated in R3 and R5 compared with R0 in all the MEAs.

For further analysis, only proteins with an abundance alteration of at least log2-fold were considered. The significance of the differential expression was evaluated also, and P<0.05 was considered to indicate a statistically significant difference. To identify the 10 proteins with the highest increases or decreases in protein expression, the average of the relative expression values in R3 and R5 of MEA A, B and C was calculated and sorted by size. The proteins with the 10 lowest and the 10 highest overall relative expression values were listed in tables (data not shown, available at https://figshare.com/s/58ffad04b1920a11fb1d).

To identify the most important targets in resistance formation, MEA A, B and C were analyzed separately and all valid values were used for further evaluation. Those proteins that followed the criteria for validity in each MEA were further analyzed. The measurement replicates of R0 were grouped (untreated) in addition to the measurement replicates of R3 and R5 (treated) and the means were compared with each other. The 15 proteins with the highest overall abundance

alterations were selected. In order to evaluate the clinical relevance of these proteins, the Kaplan-Meier Plotter (37) was used (release 2018/02/12). The relapse-free survival (RFS) in patients with luminal A breast cancer in the dataset GSE21653 was investigated.

Results

MEA mimics resistance development. Chemoresistance remains one of the primary obstacles to treating cancer. Thus, an *in vitro* model that mimics sequential treatment in the clinic was established to investigate the development of resistance to DXR. In the present study, the breast cancer cell line MCF-7 was treated with 50 nM doxorubicin for five rounds. Generally, each round consisted of a treatment phase (72 h; 50 nM DXR) and a recovery phase. The next round was initiated when cells had recovered, indicated by attaining 80% confluency. At the beginning of the MEA (R0) and subsequent to the recovery phases of R3 and R5, cells were seeded for cell viability assays and proteomic analyses. A total of three independent biological replicates were performed to investigate the process of resistance formation. These replicates were termed MEA A, B and C (Fig. 1A). Different passage numbers of the parental cells (R0) were chosen (passage 5 for MEA A, passage 7 for MEA B and passage 8 for MEA C) to compensate for possible clonal effects or cell culture artefacts. R0, R3 and R5 of the three different MEAs (A, B and C) were further analyzed. Every proteomics sample was analyzed three times and are measurement replicates in the following sections.

Development of resistance upon treatment with DXR differs in MEA A, B and C. To examine the sensitivity of the cells to 1 μM DXR, the untreated MCF-7 cells (R0), and R3 and R5 of the MEAs A, B and C, were analyzed by a cell viability assay. It was observed that resistance to DXR developed differently in each MEA (Fig. 1B). In the MEA A R3, a 1.3-fold decreased sensitivity to DXR was noted, whereas R5 displayed almost the same sensitivity to DXR as the untreated MCF-7 cells. R3 of MEA B was also 1.3-fold more resistant to treatment with DXR compared with the parental cells (R0), and the resistance was maintained in R5. MEA C, on the other hand, exhibited no resistance increase in R3, although R5 exhibited the highest increase in resistance to DXR compared with all other MEAs. These data indicated that the development of resistance to DXR in the different MEAs was neither constantly increasing nor occurring in a consistent manner.

Proteomic analysis of the treatment rounds reveals no increase in differential protein expression in later rounds. Alterations in protein expression during resistance formation were analyzed using a label-free proteomics approach. Herein, ~3,000 proteins were identified in each measurement.

To visualize the expression alterations between R0, R3 and R5 of MEA A, B and C, a scatter blot analysis was performed (Fig. 1C). In the left scatter blots, depicting the parental MCF-7 cells at different passage numbers, the spots are very close to the bisecting line of an angle, indicating that the protein expression of the untreated cells in MEA A, B and C hardly differed. The Pearson correlation values of 0.94 emphasize these results. The scatter blots in the middle panel
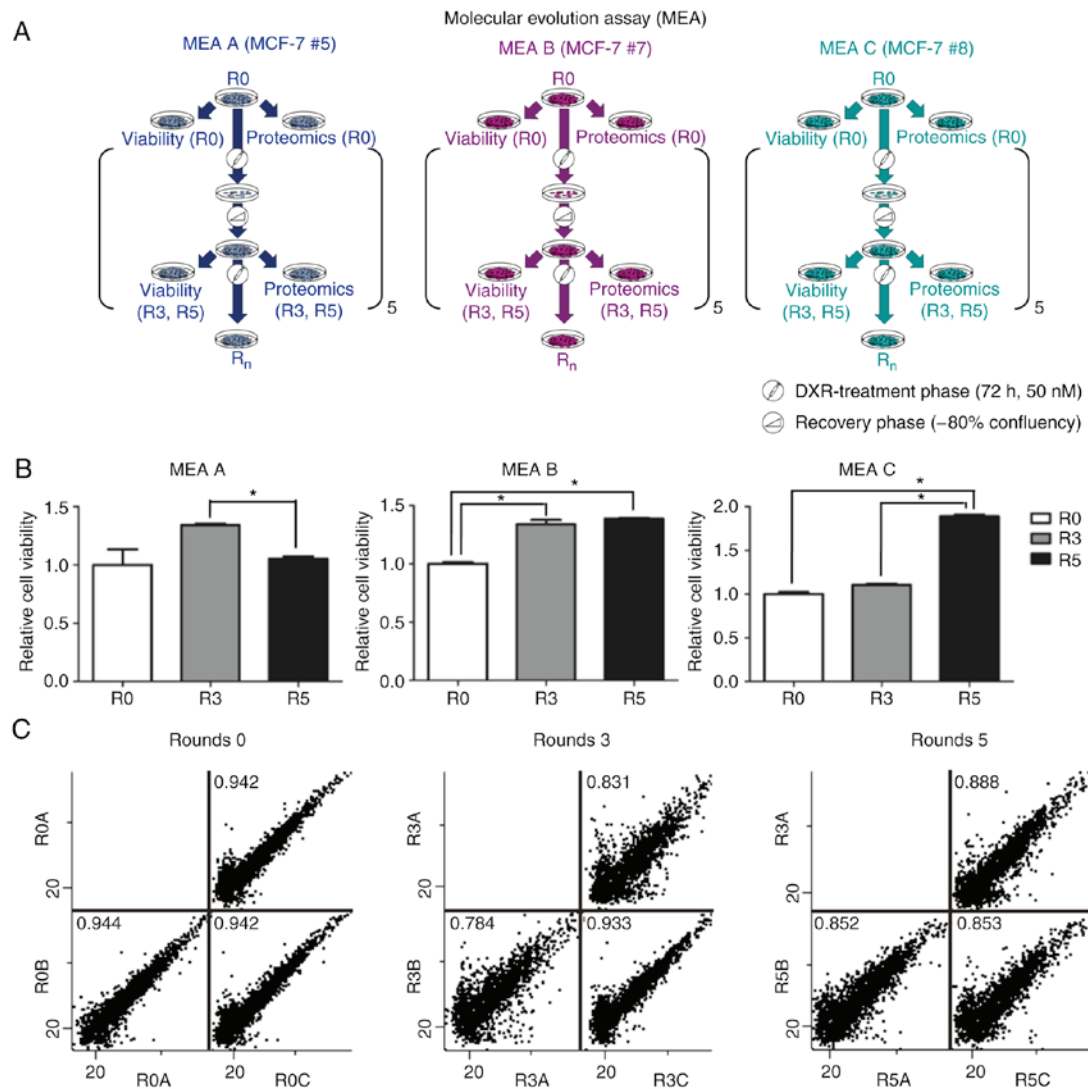
Figure 1. Introduction of the MEA. (A) Schematic representation of the MEA. MCF-7 cells were treated in five rounds (R1-R5) with 50 nM DXR for 72 h. In between the treatment rounds, the cells were allowed to recover until they reached a confluence of 80%. Three independent biological replicates were performed with cells at passage number 5, 7 and 8 (MEA A, B, C). R0, R3 and R5 were used for further analysis. (B) Analysis of resistance formation in MCF-7 cells. To evaluate the resistance formation to DXR, the MCF-7 cells of R0, R3 and R5 in MEA A, MEA B and MEA C were seeded in triplicate, treated with 1 μM doxorubicin for 72 h and subsequently analyzed by applying a CellTiter-Glo Luminescent cell viability assay. Results are presented as the mean + standard deviation. A two-tailed paired Student's t-test was performed to evaluate significance. *P<0.05. (C) Multiscatter analysis. To evaluate the similarity of the different rounds, a multiscatter analysis was performed. The median of three measurement replicates was calculated and R0, R3 and R5 of MEA A, B and C were compared with each other. A Pearson correlation index close to 1 indicates high similarity. MEA, Molecular Evolution Assay; R, round; DXR, doxorubicin.

illustrate that the spots of R3A compared with R3B, and R3A compared with R3C, diverge more from the bisector. Likewise, the Pearson correlation indices decreased. Thus, the protein expression in R3 of MEA A, B and C differed more amongst each other compared with that of the untreated cells (R0). The right panel displays the comparison of the different R5s and illustrates that the perturbation of protein expression in general was not further increased by additional treatments with DXR. Thus, it was identified that the parental cells (R0) were similar in protein expression and that a considerable perturbation was induced by three treatment rounds with DXR. A total of five treatment rounds with DXR, however, did not lead to a further increase in the difference in protein expression.

GSEA reveals signaling pathways involved in the development of resistance to DXR. To investigate the alterations in

signaling pathways involved in the development of chemoresistance in the different MEAs, a GSEA (33,34) was performed. The global ES histogram in Fig. 2A gives an overview of upregulated and downregulated proteins and illustrates that in R3 the majority of proteins were downregulated. This effect was even more marked in R5 compared with R0. For a more detailed analysis, the MEAs were examined separately. The differences in enriched gene sets are visible in the global ES histograms (data not shown; available at https://figshare.com/s/58ffad04b1920a11fb1d). Furthermore, the results were screened for GO terms and pathways known to be relevant for resistance formation (38). The normalized ES of the selected pathways exhibit alterations occurring between R0, R3 and R5 (data not shown; available at https://figshare.com/s/58ffad04b1920a11fb1d). Proteins assigned to the GO pathway 'apoptotic signaling pathway' were reduced following
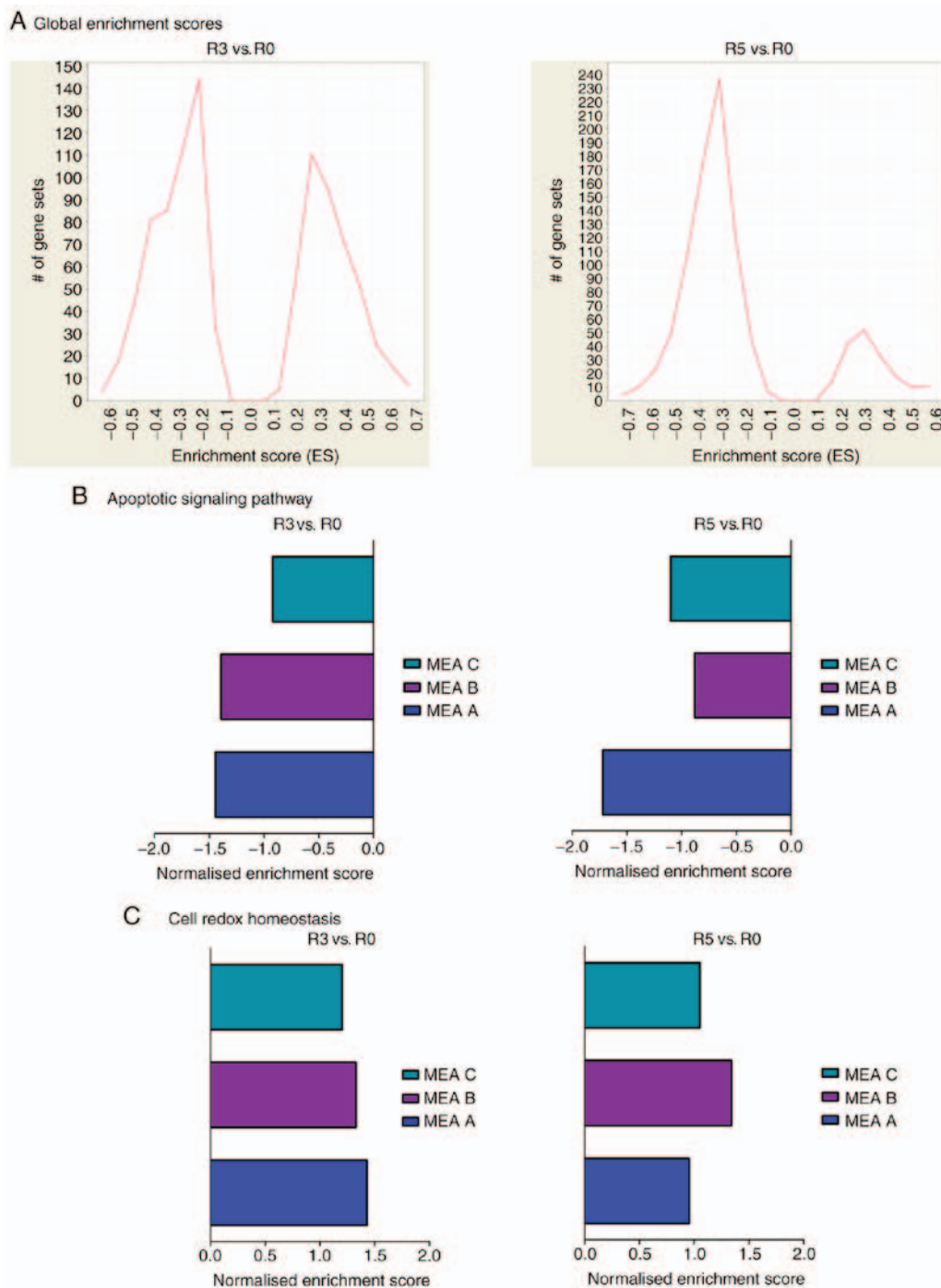
Figure 2. GSEA. GSEA was performed using gsea2-2.2.3 from the Broad Institute. (A) Global enrichment score histogram. The global enrichment score histograms are depicted to illustrate an overview of the amount of upregulated and downregulated gene sets in all the MEAs, comparing R3 and R5 with R0. (B) Apoptotic signaling pathway. The normalized enrichment score was used to facilitate the comparison of different MEAs. (C) Cell redox homeostasis. The normalized enrichment score was used to facilitate the comparison of different MEAs. GSEA, gene set enrichment analysis; R, round; MEA, Molecular Evolution Assay.

three and five treatment cycles with DXR in all MEAs. On the other hand, 'cell redox homeostasis' was generally upregulated in the DXR-treatment rounds (R3 and R5) and all MEA replicates (Fig. 2B). All other analyzed pathways, including 'locomotion', 'cell cycle', 'autophagy', 'cell motility', 'cell division', 'detoxification', 'response to toxic substance' and 'glutathione metabolic process', differed between MEA A, B and C (data not shown, available at https://figshare.com/s/58ffad04b1920a11fb1d). Therefore, all

cells in this setting escaped the chemotherapeutic selection pressure of DXR, primarily by reducing the expression of proteins belonging to the GO pathway 'apoptotic signaling pathway' and increasing the expression of the members of 'cell redox homeostasis'.

Comparing the different MEAs reveals 111 proteins with decreased and 42 proteins with increased expression in all conditions. Subsequently, the three biological replicates
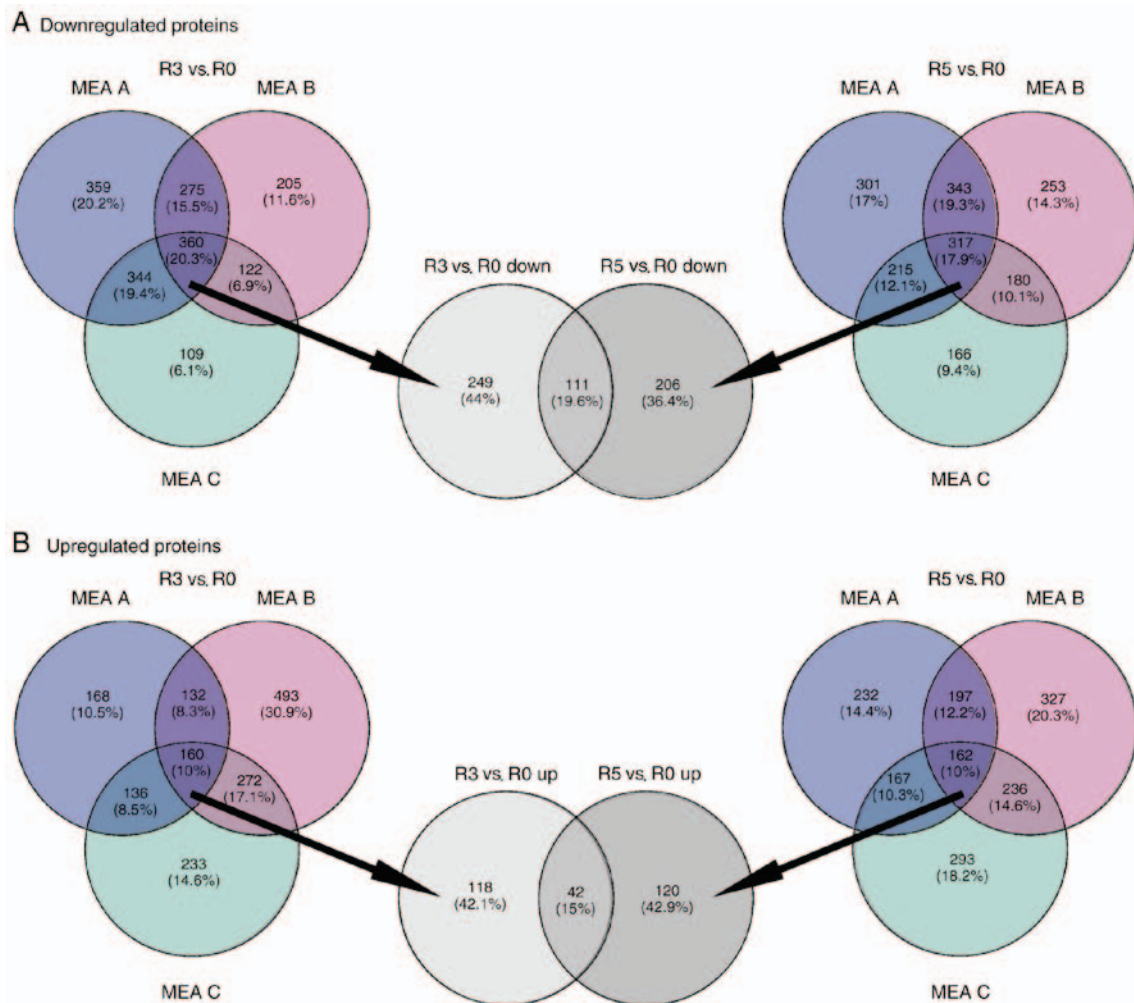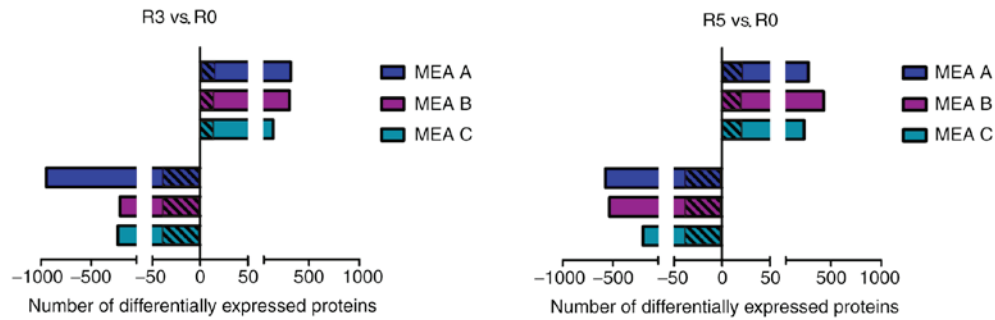
Figure 3. Comparison of MEA A, B and C. In order to compare MEA A, B and C, proteins that were identified twice in at least one group were analyzed. Missing values were replaced from a normal distribution (width, 0.3; down shift, 1.8) and a Student's t-test was performed to evaluate alterations in protein expression upon treatment with doxorubicin. Subsequently, proteins were sorted according to their t-test difference (<0, downregulated; >0, upregulated). (A) Venn diagram of downregulated proteins. To investigate the number of commonly regulated proteins between MEA A, B and C, a Venn analysis was performed. The downregulated proteins of R3 (left) and R5 (right) compared with R0 were analyzed. Proteins exhibiting decreased expression in R3 and R5 across all MEAs were again compared to elucidate which proteins were downregulated between R0 and R3 and between R0 and R5. (B) Venn diagram of upregulated proteins. The Venn diagrams illustrate the amount of commonly upregulated proteins in MEA A, B and C. Left, upregulated proteins in R3 compared with R0. Right, upregulated proteins in R5 compared with R0. Proteins with increased expression in all MEAs were compared to determine the number of continuously upregulated proteins. MEA, Molecular Evolution Assay; R, round.

(MEA A, B and C) were analyzed separately for upregulated and downregulated proteins. A total of ~1,000 proteins exhibited decreased or increased expression between R3 and R0 or R5 and R0 in each of the MEAs (Fig. 3). However, the amount of differentially expressed proteins was not consistent among the individual MEAs. To identify proteins which were commonly upregulated or downregulated in all MEAs, a Venn analysis was performed. Fig. 3A illustrates the number of proteins with reduced expression upon treatment with DXR. Following three treatment cycles with DXR, 360 proteins out of all the downregulated proteins were identical in all three MEAs (R3 vs. R0). Furthermore, 317 proteins were commonly downregulated in all MEAs following five treatment cycles with DXR (R5 vs. R0). Subsequently, these 360 proteins, which were downregulated in all MEAs following three treatment rounds with DXR, and the 317 proteins that were reduced following five treatment rounds, were compared in a further Venn diagram to determine the proteins exhibiting decreased expression in R3 and R5 compared with R0. A total of 111 proteins were commonly downregulated in all MEAs upon three and five treatment rounds with DXR. The same analysis was performed for proteins with increased expression (Fig. 3B). A total of 160 proteins were commonly upregulated in all MEAs, comparing R3 with R0. The analysis of R5 compared with R0 revealed 162 proteins with increased expression in all MEAs. The obtained proteins of R3 compared with R0 and R5 compared with R0 were further compared, and 42 proteins were detected as commonly upregulated. These upregulated and downregulated proteins are presented in tables at https://figshare.com/s/58ffad04b1920a11fb1d (data not shown). Taken together, the analysis of the protein abundance of the different MEAs revealed only a few commonly regulated proteins.

Analysis of differentially expressed proteins reveals the 20 proteins with the highest overall expression alteration.

A 1.5 Fold differentially expressed proteins

R3 vs. R0 — R5 vs. R0 (bar charts; legend: MEA A, MEA B, MEA C). Number of differentially expressed proteins.

B Proteins with highest abundance alterations

Up	R3 vs. R0						R5 vs. R0					
Genename	MEA A		MEA B		MEA C		MEA A		MEA B		MEA C	
	RE	P-value	RE	P-value	RE	P-value	RE	P-value	RE	P-value	RE	P-value
SLC3A2	2.2×10^1	1.1×10^{-5}	1.7×10^0	1.5×10^{-1}	1.6×10^0	2.4×10^{-2}	2.6×10^1	6.2×10^{-5}	1.0×10^1	2.5×10^{-5}	1.2×10^0	1.6×10^{-2}
ASS	1.1×10^1	1.1×10^{-4}	2.1×10^0	9.0×10^{-4}	1.0×10^0	9.7×10^{-1}	5.0×10^0	4.5×10^{-4}	2.1×10^1	1.3×10^{-7}	6.5×10^0	1.3×10^{-7}
BCAS1	2.8×10^1	1.3×10^{-6}	1.6×10^0	6.5×10^{-2}	4.4×10^0	3.6×10^{-2}	2.6×10^0	4.4×10^{-2}	4.6×10^0	2.2×10^{-5}	2.1×10^0	1.4×10^{-1}
KTN1	2.6×10^1	3.0×10^{-5}	3.4×10^0	5.4×10^{-3}	1.2×10^0	8.0×10^{-1}	7.2×10^0	2.5×10^{-4}	2.9×10^0	8.6×10^{-2}	1.0×10^0	9.7×10^{-1}
TFF1	1.3×10^1	1.1×10^{-2}	2.2×10^0	1.4×10^{-1}	1.4×10^0	3.8×10^{-1}	1.9×10^0	2.6×10^{-1}	7.4×10^0	1.4×10^{-3}	4.5×10^0	1.6×10^{-2}
SLC7A5	5.8×10^0	2.0×10^{-2}	2.0×10^0	1.2×10^{-1}	1.5×10^0	9.6×10^{-2}	1.7×10^0	4.4×10^{-1}	1.1×10^1	1.7×10^{-3}	1.1×10^0	6.8×10^{-1}
S100P	3.9×10^0	6.4×10^{-2}	4.0×10^0	9.1×10^{-2}	2.4×10^0	1.1×10^{-1}	1.3×10^0	8.5×10^{-1}	4.9×10^0	4.9×10^{-2}	3.4×10^0	2.2×10^{-2}
ABHD11	4.4×10^0	9.7×10^{-3}	1.1×10^0	5.8×10^{-1}	1.9×10^0	1.6×10^{-1}	2.1×10^0	3.5×10^{-2}	2.5×10^0	1.1×10^{-3}	2.2×10^0	7.3×10^{-2}
LAD1	1.0×10^0	8.1×10^{-1}	1.6×10^0	3.4×10^{-2}	1.6×10^0	3.0×10^{-1}	1.9×10^0	1.1×10^{-2}	6.0×10^0	5.7×10^{-4}	1.7×10^0	4.1×10^{-1}
PLEC	5.1×10^0	1.3×10^{-7}	1.5×10^0	1.7×10^{-4}	1.7×10^0	1.5×10^{-3}	2.6×10^0	2.6×10^{-5}	1.3×10^0	8.6×10^{-3}	1.7×10^0	1.1×10^{-3}

Down	R3 vs. R0						R5 vs. R0					
Genename	MEA A		MEA B		MEA C		MEA A		MEA B		MEA C	
	RE	P-value	RE	P-value	RE	P-value	RE	P-value	RE	P-value	RE	P-value
GFRA1	2.0×10^{-1}	3.7×10^{-5}	6.0×10^{-1}	4.7×10^{-3}	5.0×10^{-1}	5.4×10^{-2}	1.2×10^{-1}	4.5×10^{-4}	1.1×10^{-1}	8.1×10^{-4}	1.9×10^{-1}	9.8×10^{-3}
TAX1BP3	1.5×10^{-1}	6.1×10^{-4}	2.1×10^{-1}	1.3×10^{-4}	2.3×10^{-1}	1.7×10^{-1}	1.1×10^{-1}	8.7×10^{-4}	3.1×10^{-1}	1.6×10^{-1}	9.1×10^{-1}	2.5×10^{-1}
PRKAR1A	1.9×10^{-1}	7.0×10^{-4}	6.2×10^{-1}	2.9×10^{-2}	3.2×10^{-1}	5.1×10^{-3}	3.1×10^{-1}	4.5×10^{-3}	1.7×10^{-1}	1.5×10^{-2}	4.2×10^{-1}	2.2×10^{-2}
CNBP	2.5×10^{-1}	3.7×10^{-2}	4.5×10^{-1}	3.2×10^{-2}	3.0×10^{-1}	2.8×10^{-2}	4.1×10^{-1}	7.8×10^{-2}	7.7×10^{-1}	4.0×10^{-1}	1.9×10^{-1}	6.4×10^{-2}
AGR3	3.1×10^{-1}	1.3×10^{-3}	3.7×10^{-1}	1.6×10^{-3}	7.7×10^{-1}	6.9×10^{-1}	2.7×10^{-1}	2.4×10^{-3}	1.3×10^{-1}	5.6×10^{-4}	6.6×10^{-1}	5.4×10^{-1}
CA2	1.5×10^{-2}	2.5×10^{-5}	9.3×10^{-1}	1.0×10^{-2}	7.7×10^{-1}	3.7×10^{-1}	9.5×10^{-3}	7.7×10^{-5}	1.1×10^{-2}	2.7×10^{-6}	7.7×10^{-1}	6.6×10^{-2}
CMBL	4.9×10^{-1}	5.6×10^{-2}	4.7×10^{-1}	5.7×10^{-3}	4.8×10^{-1}	6.0×10^{-2}	6.5×10^{-1}	1.5×10^{-3}	7.1×10^{-2}	7.4×10^{-5}	4.3×10^{-1}	3.6×10^{-2}
NMD3	1.3×10^{-1}	1.3×10^{-4}	7.2×10^{-1}	2.7×10^{-3}	4.9×10^{-1}	6.5×10^{-2}	4.4×10^{-1}	1.2×10^{-2}	2.5×10^{-1}	4.7×10^{-4}	5.7×10^{-1}	1.1×10^{-1}
PNPO	4.3×10^{-1}	2.1×10^{-2}	7.7×10^{-1}	2.3×10^{-1}	2.5×10^{-1}	6.2×10^{-2}	9.6×10^{-2}	9.4×10^{-5}	5.8×10^{-1}	1.7×10^{-1}	5.9×10^{-1}	4.3×10^{-4}
TPD52L2	2.8×10^{-1}	1.5×10^{-3}	7.9×10^{-1}	1.1×10^{-2}	3.9×10^{-1}	1.5×10^{-1}	2.3×10^{-1}	1.6×10^{-2}	9.3×10^{-1}	3.6×10^{-1}	3.6×10^{-1}	2.6×10^{-1}

Figure 4. Differentially expressed proteins. For a comparison of MEA A, B and C only proteins that were identified twice in at least one group were considered. Missing values were imputed (width, 0.3; down shift, 1.8). In order to determine the alterations in protein expression during resistance formation, a Student's t-test was performed and R3 vs. R0 and R5 vs. R0 were compared. Only proteins exhibiting a Student's t-test difference of at least |0.6| (1.5 fold) were further examined. The proteins with decreased expression levels are presented as negative values, and vice versa. (A) Number of differentially expressed proteins. The differentially expressed proteins of R3 (left) and R5 (right) compared with R0 were analyzed. The hatched area represents the commonly regulated proteins. (B) Proteins with the highest abundance alterations. The depicted tables illustrate the proteins with the highest abundance alterations across all MEAs. In the upper table the 10 proteins with the largest overall increase in expression are presented. The lower table displays the 10 proteins with the greatest reduction in expression upon treatment with doxorubicin. A two-tailed student's t-test with a false discovery rate of 0.05 was used to compare R3 with R0 and R5 with R0. $P<0.05$ was considered to indicate a statistically significant difference. MEA, Molecular Evolution Assay; R, round; RE, relative expression.

Subsequently, the three MEAs were analyzed separately for differentially expressed proteins, with a threshold of a 1.5-fold change. This led numbers of downregulated proteins between R3 and R0 of 946 in MEA A, 212 in MEA B and 233 in MEA C. A smaller number of proteins were upregulated: 318 in MEA A, 307 in MEA B and 146 in MEA C.

Regarding alterations in protein expression comparing R5 to R0, it was observed that 851 proteins in MEA A, 960 in MEA B and 435 in MEA C were differentially expressed. Only 4-7% of all identified and differentially expressed proteins were commonly regulated in all MEAs (Fig. 4A hatched area).
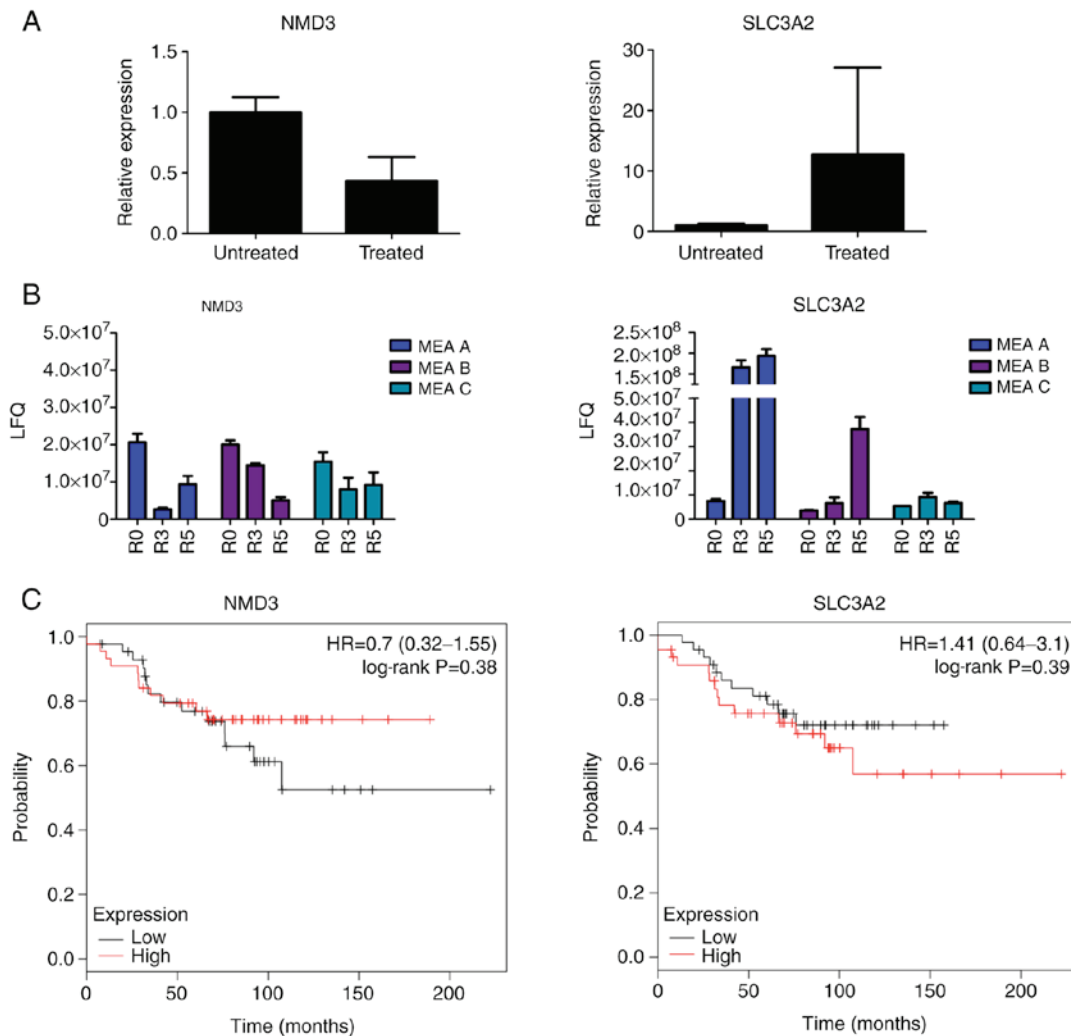
Figure 5. Potential common drivers of chemoresistance. Treated cells (R3 and R5) were compared with untreated cells (R0) to identify proteins that were commonly regulated during resistance formation across all MEAs. NMD3 and SLC3A2 are presented as representative examples. (A) Global comparison of treated and untreated cells. All values are depicted as relative expression values normalized to untreated cells, and are presented as the mean + standard deviation of all MEAs. (B) Detailed analysis of each MEA. The LFQ values of each round are depicted here as the mean + standard deviation of the measurement replicates. (C) Kaplan-Meier plots. The relapse-free survival of luminal A breast cancer patients was analyzed using the GSE21653 dataset. MEA, Molecular Evolution Assay; R, round; NMD3, 60S ribosomal export protein NMD3; SLC3A2, 4F2 cell-surface antigen heavy chain; LFQ, label free quantification.

In Fig. 4B, the 20 proteins with the highest overall abundance alterations are depicted, displaying their relative expression and the respective P-values.

Commonly regulated proteins are likely to be associated with chemoresistance. In order to identify the most promising targets in the development of chemoresistance, treated samples (R3 and R5) were compared with untreated samples (R0) across all three MEAs. The proteins which were present in all MEAs (A, B and C) were further analyzed, according to their differential expression. Finally, 15 proteins with the highest overall expression alterations are presented in a table at https://figshare.com/s/58ffad04b1920a11fb1d (data not shown). The majority of these proteins are known to be involved in crucial mechanisms and pathways, including tumorigenesis, the cell cycle and apoptosis. A total of two representative proteins are presented in Fig. 5. 60S ribosomal export protein NMD3 (NMD3) is a representative example of proteins which were downregulated upon treatment with DXR in every MEA

and exhibited a decrease in protein expression. On the other hand, 4F2 cell-surface antigen heavy chain (SLC3A2) was upregulated 12.7-fold on average, and represents an example of increasing proteins expression levels (Fig. 5A). The detailed alteration in expression of these targets in the individual MEAs and rounds is displayed in Fig. 5B. The individual expression levels overall followed a similar trend throughout the MEAs: Reduced expression following treatment with DXR in the case of NMD3, and an increase in SLC3A2. This indicated the importance of these proteins in resistance development. To further evaluate the impact of these proteins on cancer progression, the RFS of a cohort of patients with breast cancer (luminal A tumors) was investigated *in silico* using a Kaplan-Meier analysis provided by Kaplan-Meier Plotter (37). Breast tumors with low NMD3 expression levels recurred earlier [hazard ratio (HR)=0.7] compared with tumors exhibiting high NMD3 expression. In line with the present proteomic analysis, high expression levels of SLC3A2 led to shorter RFS periods in comparison with tumors with low SLC3A2 expression (HR=1.4; Fig. 5C).

Discussion

Drug resistance remains one of the principal obstacles in the treatment of cancer and frequently correlates with tumor relapse, in addition to poor patient outcomes. In the present study, the development of chemoresistance was investigated using a proteomics approach, to acquire a comprehensive analysis of the fundamental factors, patterns and mechanisms.

To generate chemoresistance, other studies (23-29) have maintained cells in DXR-containing medium, whereas in the present study, to the best of our knowledge for the first time, cells were treated in rounds with treatment-free periods and were subsequently analyzed with proteomics. Persistent treatment with DXR leads to a continuous upregulation or downregulation of proteins compensating for the permanent toxic stress, similar to multiple drug resistance mechanisms, including the upregulation of 5'-adenosine triphosphate-binding cassette transporters (23-29). In the present assay, the temporary absence of the selection pressure caused further perturbations in protein expression. This increased the complexity of the resistance model. The removal of DXR leads to regrowth of surviving cells in which the fittest clones with the highest proliferation rate have the highest impact on the composition of the recurrent tumor cell population. Therefore, it was hypothesized that the MEA was more reflective of the therapeutic regimen in the clinic. Analyzing resistance formation by MEA may thus lead to novel insights.

The development of chemoresistance in tumors may generally be explained by two hypotheses: The CSC model and the clonal evolution model (14-19). Choi et al (39) reported that only 1.2% of wild type MCF-7 cells exhibit a CSC-like phenotype. If only these CSCs had survived the treatment, a more homogenous protein pattern, in addition to an increase in stem cell markers, may have been detected in the present study. Therefore, it may be hypothesized that CSCs have only a minor impact on the development of chemoresistance in the present setting, and the clonal evolution model may therefore be favored for the present *in vitro* resistance assay. There are numerous pathways involved in drug resistance (23-28) in which proteins were not observed to be altered in the present study. A possible reason may be conditions of this assay, for example with recovery phases and sequential treatment. Another reason may be the performed proteomic analysis. The analysis of differentially expressed proteins with the present method has a number of advantages compared with frequently used genomics methods. However, it is not possible to perform a comprehensive analysis due to limitations in detecting the entirety of human proteins. Furthermore, the applied proteomic analysis is not able to detect alterations in mRNA expression levels, which a number of publications have investigated (27,28). Furthermore, it has been reported that there is only a very weak correlation between mRNA expression levels and protein expression (40). However, protein expression is responsible for the manifestation of biological phenotypes and, therefore, a proteomics approach may be the superior analysis for the evaluation of resistance formation. By applying the label-free LC-MS technique in the present study, 3,000 of the 30,057 human proteins (41) were identified, a notable improvement compared with previous studies (25,42,43). Also, stringent cut-off criteria were chosen to minimize the detection of false positive results.

For an unbiased analysis, a GSEA was utilized. Common resistance mechanisms, including 'apoptotic signaling pathway' and 'cell redox homeostasis' were demonstrated to be altered. A reduction in apoptosis is a common mechanism through which to escape cell death, and has been reported in previous studies (44,45). Particularly in the context of treatment with DXR, the increased expression of proteins regulating cell redox homeostasis is plausible. This pathway analysis further demonstrated that the development of resistance to DXR differed in each MEA.

By comparing treated (R3 and R5) with untreated cells (R0) of all MEAs, NMD3 and SLC3A2 were identified to be representative examples of downregulated or upregulated proteins, respectively. SLC3A2 is associated with cell survival, migration and tumor growth in renal cancer, and may thus be a promising resistance marker in breast cancer (46,47). Additionally, NMD3 has a marked impact on RNA biosynthesis, particularly ribosomal RNA synthesis, and may therefore influence tumorigenesis in general (48); however, a direct role for this protein in chemoresistance remains to be elucidated.

The results of the present study demonstrated through the commonly upregulated or downregulated targets that the development of chemoresistance differed in each MEA. Thus, only a few general drivers of resistance formation were identified (4-7% of the identified proteins) and >90% of the differentially expressed proteins were altered only in one of the assays. This phenomenon may be caused, on the one hand, by slightly heterogeneous initial protein expression due to pre-existing genomic instability and, on the other hand, by the treatment with DXR, which had the highest impact on the perturbation of differentially expressed proteins in MEA A, B and C. It was not possible to detect a dominant pattern of differential protein expression which was reproducibly present in all replicates. The assay conditions and analyses also did not allow for the drawing of conclusions as to whether resistance formation is a stochastic or, at least, a multi-directed process, as an increased number of replicates may identify patterns in resistance formation. Furthermore, it was observed that the sensitivity to DXR varied in each MEA during the five treatment rounds. Chemoresistance is defined as the insensitivity of tumor cells to chemotherapeutic drugs, leading to tumor progression during chemotherapy (49). However, the underlying mechanisms are different. One such mechanism is intrinsic drug resistance; this means that tumor cells are resistant to the applied drug from the beginning of treatment. The other mechanism is acquired resistance, wherein tumor cells develop resistance to the applied drug following an initial response (50). In the present study, it was observed that in MEA A, for example, five times-treated cells exhibited the same sensitivity to DXR as untreated cells. This indicated that five treatment rounds with DXR did not further increase resistance compared with three times-treated cells, and also that resistance may not be a persistent condition. Furthermore, it was demonstrated that five treatment rounds altered protein expression while not necessarily increasing resistance to the applied drug. This observed effect may be due to clonal selection, which favors faster growing cell clones that then represent the majority of cells in the recovery phase. Thus, the present assay did not select for the most resistant clones; rather, for those that survived the treatment and were subsequently able

to repopulate. This resembles the situation in the clinic more accurately than maintaining a constant selection pressure.

Additionally, the diversity in the development of resistance may be due to the heterogeneity of tumor cells. According to The Cancer Genome Atlas and the International Cancer Genome Consortium, estrogen receptor positive (ER$^+$) breast cancer exhibits the greatest diversity concerning gene expression, mutations, alterations in copy numbers and patient outcomes (51-53). Thus, it may be hypothesized that the response to chemotherapy may differ in each patient. This may lead to varying selection of resistant clones, which give rise to metastases and recurrent tumors. It was previously reported that disseminating breast cancer cells exhibit a different gene expression pattern and an increased resistance to chemotherapeutics compared with the primary tumor (54-59). Furthermore, Folgueira *et al* (60) demonstrated, by comparing ER$^+$ breast tumor samples pre- and post-treatment with DXR and cyclophosphamide, that 389 genes were differentially expressed.

Another general reason for the heterogeneity of tumors is genomic instability, a hallmark of cancer (20). Tomasetti *et al* (61) reported that the majority of mutations leading to tumorigenesis are random DNA replication errors, aside from hereditary and environmental mutations. This finding indicated that every patient with breast cancer may exhibit a different response to therapy, RFS and overall survival.

In conclusion, the present *in vitro* model indicated that the development of chemoresistance is a multi-directed or varying process. Due to the genomic instability in breast cancer, the response to chemotherapeutics, and thus the development of resistance by clonal selection, may be an event that rarely follows certain patterns. Transferred to the clinical setting with even more perturbations in resistance formation, these results may explain why cancer remains difficult to treat and why the patient outcome is hard to predict. This furthers emphasizes the requirement for an individual diagnosis of resistance markers, in addition to patient-tailored therapy.

Availability of data and materials

The datasets generated and analyzed during the current study are available at https://figshare.com/s/58ffad04b1920a11fb1d, DOI: 10.6084/m9.figshare.5960887.

Authors' contributions

AS analyzed the proteomics data, performed the pathway analysis and wrote the manuscript. AH performed cell culture experiments and sample preparations for proteomics. BL provided support in presenting and discussing the data. TF conducted the LC-MS experiments and assisted with data analysis. EW and GJA provided conceptual advice. AR conceived the study and wrote the manuscript. All authors commented on the final manuscript and conclusions of this work.

Ethics approval and consent to participate

Not applicable.

Patient consent for publication

Not applicable.

Competing interests

The authors declare that they have no competing interests.

References

1. American Cancer Society: Cancer facts & figures 2018. American Cancer Society, 2018.
2. Globocan: Cancer today. International Agency for Research on Cancer, 2012.
3. Miller KD, Siegel RL, Lin CC, Mariotto AB, Kramer JL, Rowland JH, Stein KD, Alteri R and Jemal A: Cancer treatment and survivorship statistics, 2016. CA Cancer J Clin 66: 271-289, 2016.
4. Arcamone F, Cassinelli G, Fantini G, Grein A, Orezzi P, Pol C and Spalla C: Adriamycin, 14-hydroxydaunomycin, a new antitumor antibiotic from S. peucetius var. caesius. Biotechnol Bioeng 11: 1101-1110, 1969.
5. Tewey KM, Rowe TC, Yang L, Halligan BD and Liu LF: Adriamycin-induced DNA damage mediated by mammalian DNA topoisomerase II. Science 226: 466-468, 1984.
6. Chen NT, Wu CY, Chung CY, Hwu Y, Cheng SH, Mou CY and Lo LW: Probing the dynamics of doxorubicin-DNA intercalation during the initial activation of apoptosis by fluorescence lifetime imaging microscopy (FLIM). PLoS One 7: e44947, 2012.
7. Mizutani H, Tada-Oikawa S, Hiraku Y, Kojima M and Kawanishi S: Mechanism of apoptosis induced by doxorubicin through the generation of hydrogen peroxide. Life Sci 76: 1439-1453, 2005.
8. Hilmer SN, Cogger VC, Muller M and Le Couteur DG: The hepatic pharmacokinetics of doxorubicin and liposomal doxorubicin. Drug Metab Dispos 32: 794-799, 2004.
9. Gewirtz DA: A critical evaluation of the mechanisms of action proposed for the antitumor effects of the anthracycline antibiotics adriamycin and daunorubicin. Biochem Pharmacol 57: 727-741, 1999.
10. Minotti G, Menna P, Salvatorelli E, Cairo G and Gianni L: Anthracyclines: Molecular advances and pharmacologic developments in antitumor activity and cardiotoxicity. Pharmacol Rev 56: 185-229, 2004.
11. Tacar O, Sriamornsak P and Dass CR: Doxorubicin: An update on anticancer molecular action, toxicity and novel drug delivery systems. J Pharm Pharmacol 65: 157-170, 2013.
12. Benchekroun MN, Sinha BK and Robert J: Doxorubicin-induced oxygen free radical formation in sensitive and doxorubicin-resistant variants of rat glioblastoma cell lines [corrected and republished erratum originally printed in FEBS Lett 1993 May 17;322(3):295-8]. FEBS Lett 326: 302-305, 1993.
13. Early Breast Cancer Trialists' Collaborative Group (EBCTCG); Peto R, Davies C, Godwin J, Gray R, Pan HC, Clarke M, Cutter D, Darby S, McGale P, Taylor C, *et al*: Comparisons between different polychemotherapy regimens for early breast cancer: Meta-analyses of long-term outcome among 100,000 women in 123 randomised trials. Lancet 379: 432-444, 2012.
14. Meacham CE and Morrison SJ: Tumour heterogeneity and cancer cell plasticity. Nature 501: 328-337, 2013.
15. Greaves M and Maley CC: Clonal evolution in cancer. Nature 481: 306-313, 2012.
16. Shackleton M, Quintana E, Fearon ER and Morrison SJ: Heterogeneity in cancer: Cancer stem cells versus clonal evolution. Cell 138: 822-829, 2009.

17. Cairns J: Mutation selection and the natural history of cancer. Nature 255: 197-200, 1975.
18. Nowell PC: The clonal evolution of tumor cell populations. Science 194: 23-28, 1976.
19. Kopp F, Hermawan A, Oak PS, Ulaganathan VK, Herrmann A, Elnikhely N, Thakur C, Xiao Z, Knyazev P, Ataseven B, et al: Sequential salinomycin treatment results in resistance formation through clonal selection of epithelial-like tumor cells. Transl Oncol 7: 702-711, 2014.
20. Hanahan D and Weinberg RA: Hallmarks of cancer: The next generation. Cell 144: 646-674, 2011.
21. Turner NC and Reis-Filho JS: Genetic heterogeneity and cancer drug resistance. Lancet Oncol 13: e178-e185, 2012.
22. Bedard PL, Hansen AR, Ratain MJ and Siu LL: Tumour heterogeneity in the clinic. Nature 501: 355-364, 2013.
23. Bankusli I, Yin MB, Mazzoni A, Abdellah AJ and Rustum YM: Enhancement of adriamycin-induced cytotoxicity by increasing retention and inhibition of DNA repair in DOX-resistant P388 cell lines with new calcium channel blocker, DMDP. Anticancer Res 9: 567-574, 1989.
24. de Jong S, Zijlstra JG, de Vries EG and Mulder NH: Reduced DNA topoisomerase II activity and drug-induced DNA cleavage activity in an adriamycin-resistant human small cell lung carcinoma cell line. Cancer Res 50: 304-309, 1990.
25. Wang Z, Liang S, Lian X, Liu L, Zhao S, Xuan Q, Guo L, Liu H, Yang Y, Dong T, et al: Identification of proteins responsible for adriamycin resistance in breast cancer cells using proteomics analysis. Sci Rep 5: 9301, 2015.
26. Gehrmann ML, Fenselau C and Hathout Y: Highly altered protein expression profile in the adriamycin resistant MCF-7 cell line. J Proteome Res 3: 403-409, 2004.
27. Aas T, Børresen AL, Geisler S, Smith-Sørensen B, Johnsen H, Varhaug JE, Akslen LA and Lønning PE: Specific P53 mutations are associated with de novo resistance to doxorubicin in breast cancer patients. Nat Med 2: 811-814, 1996.
28. Gottesman MM: Mechanisms of cancer drug resistance. Annu Rev Med 53: 615-627, 2002.
29. Hermawan A, Wagner E and Roidl A: Consecutive salinomycin treatment reduces doxorubicin resistance of breast tumor cells by diminishing drug efflux pump expression and activity. Oncol Rep 35: 1732-1740, 2016.
30. Kopp F, Oak PS, Wagner E and Roidl A: miR-200c sensitizes breast cancer cells to doxorubicin treatment by decreasing TrkB and Bmi1 expression. PLoS One 7: e50469, 2012.
31. Tyanova S, Temu T, Carlson A, Sinitcyn P, Mann M and Cox J: Visualization of LC-MS/MS proteomics data in MaxQuant. Proteomics 15: 1453-1456, 2015.
32. Tyanova S, Temu T, Sinitcyn P, Carlson A, Hein MY, Geiger T, Mann M and Cox J: The perseus computational platform for comprehensive analysis of (prote)omics data. Nat Methods 13: 731-740, 2016.
33. Subramanian A, Tamayo P, Mootha VK, Mukherjee S, Ebert BL, Gillette MA, Paulovich A, Pomeroy SL, Golub TR, Lander ES, et al: Gene set enrichment analysis: A knowledge-based approach for interpreting genome-wide expression profiles. Proc Natl Acad Sci USA 102: 15545-15550, 2005.
34. Mootha VK, Lindgren CM, Eriksson KF, Subramanian A, Sihag S, Lehar J, Puigserver P, Carlsson E, Ridderstråle M, Laurila E, et al: PGC-1alpha-responsive genes involved in oxidative phosphorylation are coordinately downregulated in human diabetes. Nat Genet 34: 267-273, 2003.
35. Ashburner M, Ball CA, Blake JA, Botstein D, Butler H, Cherry JM, Davis AP, Dolinski K, Dwight SS, Eppig JT, et al: Gene ontology: Tool for the unification of biology. The gene ontology consortium. Nat Genet 25: 25-29, 2000.
36. Oliveros JC: Venny. An interactive tool for comparing lists with Venn's diagrams. 2007-2015.
37. Györffy B, Lanczky A, Eklund AC, Denkert C, Budczies J, Li Q and Szallasi Z: An online survival analysis tool to rapidly assess the effect of 22,277 genes on breast cancer prognosis using microarray data of 1,809 patients. Breast Cancer Res Treat 123: 725-731, 2010.
38. Shibue T and Weinberg RA: EMT, CSCs, and drug resistance: The mechanistic link and clinical implications. Nat Rev Clin Oncol 14: 611-629, 2017.
39. Choi HS, Kim DA, Chung H, Park IH, Kim BH, Oh ES and Kang DH: Screening of breast cancer stem cell inhibitors using a protein kinase inhibitor library. Cancer Cell Int 17: 25, 2017.
40. Pertea M: The human transcriptome: An unfinished story. Genes 3: 344-360, 2012.
41. Kim MS, Pinto SM, Getnet D, Nirujogi RS, Manda SS, Chaerkady R, Madugundu AK, Kelkar DS, Isserlin R, Jain S, et al: A draft map of the human proteome. Nature 509: 575-581, 2014.
42. Holm M, Saraswat M, Joenväärä S, Ristimäki A, Haglund C and Renkonen R: Colorectal cancer patients with different C-reactive protein levels and 5-year survival times can be differentiated with quantitative serum proteomics. PLoS One 13: e0195354, 2018.
43. Koplev S, Lin K, Dohlman AB and Ma'ayan A: Integration of pan-cancer transcriptomics with RPPA proteomics reveals mechanisms of epithelial-mesenchymal transition. PLoS Comput Biol 14: e1005911, 2018.
44. Marin JJ, Al-Abdulla R, Lozano E, Briz O, Bujanda L, Banales JM and Macias RI: Mechanisms of resistance to chemotherapy in gastric cancer. Anticancer Agents Med Chem 16: 318-334, 2016.
45. Pfeffer CM and Singh ATK: Apoptosis: A target for anticancer therapy. Int J Mol Sci 19: E448, 2018.
46. Poettler M, Unseld M, Braemswig K, Haitel A, Zielinski CC and Prager GW: CD98hc (SLC3A2) drives integrin-dependent renal cancer cell behavior. Mol Cancer 12: 169, 2013.
47. Prager GW, Poettler M, Schmidinger M, Mazal PR, Susani M, Zielinski CC and Haitel A: CD98hc (SLC3A2), a novel marker in renal cell cancer. Eur J Clin Invest 39: 304-310, 2009.
48. Bai B, Moore HM and Laiho M: CRM1 and its ribosome export adaptor NMD3 localize to the nucleolus and affect rRNA synthesis. Nucleus 4: 315-325, 2013.
49. Schwab M: Encyclopedia of cancer. Springer, Heidelberg, 2011.
50. Sommer AK, Hermawan A, Mickler FM, Ljepoja B, Knyazev P, Bräuchle C, Ullrich A, Wagner E and Roidl A: Salinomycin co-treatment enhances tamoxifen cytotoxicity in luminal A breast tumor cells by facilitating lysosomal degradation of receptor tyrosine kinases. Oncotarget 7: 50461-50476, 2016.
51. Cancer Genome Atlas Network: Comprehensive molecular portraits of human breast tumours. Nature 490: 61-70, 2012.
52. Nik-Zainal S, Davies H, Staaf J, Ramakrishna M, Glodzik D, Zou X, Martincorena I, Alexandrov LB, Martin S, Wedge DC, et al: Landscape of somatic mutations in 560 breast cancer whole-genome sequences. Nature 534: 47-54, 2016.
53. Parker JS, Mullins M, Cheang MC, Leung S, Voduc D, Vickery T, Davies S, Fauron C, He X, Hu Z, et al: Supervised risk predictor of breast cancer based on intrinsic subtypes. J Clin Oncol 27: 1160-1167, 2009.
54. Goswami S, Wang W, Wyckoff JB and Condeelis JS: Breast cancer cells isolated by chemotaxis from primary tumors show increased survival and resistance to chemotherapy. Cancer Res 64: 7664-7667, 2004.
55. Goswami S, Philippar U, Sun D, Patsialou A, Avraham J, Wang W, Di Modugno F, Nistico P, Gertler FB and Condeelis JS: Identification of invasion specific splice variants of the cytoskeletal protein Mena present in mammary tumor cells during invasion in vivo. Clin Exp Metastasis 26: 153-159, 2009.
56. Patsialou A, Wang Y, Lin J, Whitney K, Goswami S, Kenny PA and Condeelis JS: Selective gene-expression profiling of migratory tumor cells in vivo predicts clinical outcome in breast cancer patients. Breast Cancer Res 14: R139, 2012.
57. Wang W, Wyckoff JB, Wang Y, Bottinger EP, Segall JE and Condeelis JS: Gene expression analysis on small numbers of invasive cells collected by chemotaxis from primary mammary tumors of the mouse. BMC Biotechnol 3: 13, 2003.
58. Wyckoff JB, Segall JE and Condeelis JS: The collection of the motile population of cells from a living tumor. Cancer Res 60: 5401-5404, 2000.
59. Yates LR, Knappskog S, Wedge D, Farmery JHR, Gonzalez S, Martincorena I, Alexandrov LB, Van Loo P, Haugland HK, Lilleng PK, et al: Genomic evolution of breast cancer metastasis and relapse. Cancer Cell 32: 169-184.e7, 2017.
60. Koike Folgueira MA, Brentani H, Carraro DM, De Camargo Barros Filho M, Hirata Katayama ML, Santana de Abreu AP, Mantovani Barbosa E, De Oliveira CT, Patrão DF, Mota LD, et al: Gene expression profile of residual breast cancer after doxorubicin and cyclophosphamide neoadjuvant chemotherapy. Oncol Rep 22: 805-813, 2009.
61. Tomasetti C, Li L and Vogelstein B: Stem cell divisions, somatic mutations, cancer etiology, and cancer prevention. Science 355: 1330-1334, 2017.